GEOPHYSICAL RESEARCH LETTERS, VOL. 35, L24801, doi:10.1029/2008GL036279, 2008

Retrievals of aerosol single-scattering albedo and effective aerosol layer height for biomass-burning smoke: Synergy derived from "A-Train" sensors

Myeong-Jae Jeong[1,2] and N. Christina Hsu[2]

Received 8 October 2008; accepted 13 November 2008; published 18 December 2008.

[1] In this paper, we present results from a new algorithm which provides aerosol layer height (ALH) as well as single-scattering albedo (SSA) for biomass-burning smoke aerosols by merging measurements from three of the "A-Train" satellite sensors: MODIS, OMI, and CALIOP. This algorithm has been applied successfully to biomass burning episodes over North America and Southeast Asia, and the corresponding SSA retrievals show good agreement with those from the AERONET. Furthermore, by combining ALH information from CALIOP with the retrieved SSA, extended information of ALH over wide areas can be obtained outside the CALIPSO track. Even when CALIPSO data are not available, this algorithm will still allow for the separation of aerosols residing within the boundary layer from those elevated in the free troposphere by combining only MODIS and OMI data. Results from this study will provide a better understanding of the height of smoke layers generated from biomass burning and thus improve aerosol models and the prediction of smoke aerosol transport.
Citation: Jeong, M.-J., and N. C. Hsu (2008), Retrievals of aerosol single-scattering albedo and effective aerosol layer height for biomass-burning smoke: Synergy derived from "A-Train" sensors, *Geophys. Res. Lett.*, *35*, L24801, doi:10.1029/2008GL036279.

1. Introduction

[2] A new era in aerosol-related studies began with the launch of state-of-the-art satellite sensors designed with aerosol remote sensing in mind. These sensors fly onboard a well-coordinated observing system, called the "A-Train" (Afternoon satellite constellation) [*NASA*, 2003], consisting of an array of satellites flying in formation. The capabilities of the individual sensors aboard these satellites are complementary and overlapping in terms of retrievable aerosol parameters, sensitivity, spatial resolution, and coverage [*Anderson et al.*, 2005]. The ability to obtain value-added information about aerosols by merging measurements from this system has been greatly increased.

[3] In the visible bands, the upwelling radiance that would be measured at the top of the atmosphere (TOA) is nearly independent of the height of aerosol plumes so that their loading (e.g., aerosol optical thickness; AOT) can be derived relatively accurately from satellites as long as cloud-screening and surface reflectance characterization are valid [e.g., *Jeong et al.*, 2005]. Conversely, the upwelling UV radiance at TOA is very sensitive to the height and absorption of aerosols in addition to their loading [e.g., *Hsu et al.*, 1999] such that inferring AOT only from TOA UV radiance used to be a significantly under-determined problem. However, such sensitivity of UV radiance brings us an opportunity that we can derive aerosol absorption by an attempt to close the TOA UV radiance if information on aerosol loading and height is provided, or vice versa. These closures are now possible given the "A-Train": aerosol loading (AOT) from MODerate resolution Imaging Spectrophotometer (MODIS) on Aqua, UV spectra from Ozone Monitoring Instrument (OMI) aboard Aura, and aerosol layer height (ALH) from Cloud-Aerosol Lidar with Orthogonal Polarization (CALIOP) onboard the Cloud-Aerosol Lidar and Infrared Pathfinder Satellite Observation (CALIPSO) satellite. In this paper, we introduce a new algorithm for deriving the single-scattering albedo (SSA) of biomass-burning smoke (BBS) aerosols by merging such measurements from the "A-Train" satellite sensors, and discuss how they can be used as a robust spread function to ALH information outside the CALIPSO path over MODIS granules.

2. Data and Methodology

[4] The new algorithm, hereinafter, will be referred to as "A-Train" Aerosol Single-scattering albedo and layer Height Estimation algorithm, or briefly as ASHE algorithm. The algorithm takes advantage of the aforementioned sensitivity of the TOA UV spectra (e.g., UV aerosol index, or UV AI) to changes in ALH and SSA. The UV AI derived from TOMS has been used for more than a decade to detect UV-absorbing aerosols [e.g., *Hsu et al.*, 1996; *Jeong and Li*, 2005], and its dependency on AOT, SSA and ALH has been well characterized [*Herman et al.*, 1997; *Torres et al.*, 1998; *Hsu et al.*, 1999]. In this study, the UV AI is calculated from the radiances at 331 nm and 361 nm measured from the OMI UV-2 sensor. It is defined as

$$AI(\tau_a, \omega_0, z_a) = -100^* \left\{ \log_{10}\left[\left(\frac{I_{331}}{I_{360}}\right)_{meas}\right] - \log_{10}\left[\left(\frac{I_{331}}{I_{360}}\right)_{calc}\right] \right\}, \quad (1)$$

where I_{meas} and I_{calc} are the measured and calculated TOA upwelling radiances, respectively, at a given wavelength using a Lambert-equivalent reflectivity derived at 360 nm, and τ_a, ω_0, and z_a represent AOT, SSA, and ALH, respectively. In principle, SSA can be estimated if AI,

[1]Goddard Earth Science and Technology Center, University of Maryland Baltimore County, Baltimore, Maryland, USA.
[2]NASA Goddard Space Flight Center, Greenbelt, Maryland, USA.

0094-8276/08/2008GL036279$05.00

AOT, and ALH are known under a reasonable assumption on aerosol size (or spectral dependency of AOT). With the same token, ALH can be inferred when AI, AOT, and SSA are known.

[5] We use AOT (550 nm) and Ångström exponent (470/660 nm pair) values from the MODIS Collection 5 Level 2 aerosol products to provide the ASHE algorithm with constraints of aerosol loading and size, respectively. The OMI Level 1B radiance product (Version 3) is utilized to derive UV AI as described above. We also exploit the CALIPSO Level 2 Vertical Feature Mask (VFM) product to obtain ALH to be fed to ASHE algorithm for retrieving SSA along the CALIPSO tracks. The VFM product provides a vertical mapping of the locations of aerosols and clouds together with the information about the types of each layer [*Vaughan et al.*, 2005]. Given the accuracy of the CALIOP altitude registration, the locations of the layer identified in the VFM products are expected to be very accurate (30–60 meters in the troposphere). Discrimination between aerosols and clouds is in general expected to be reasonably good in the VFM product (cf. http://eosweb.larc.nasa.gov/PRODOCS/calipso/Quality_Summaries/), except for conditions (1) when very dense layers of aerosol such as dust or smoke are close to the source areas and (2) in heterogeneous layers where aerosols are very close to or mixed with clouds. In this paper, the value of ALH from CALIPSO is defined as the median altitude of aerosol layers identified in the VFM data so that it is consistent with the ALH from the ASHE algorithm, which assumes a Gaussian distribution for aerosol vertical profile.

[6] Given the information about aerosol loading (AOT), size (Ångström exponent), and ALH from the datasets mentioned above, only aerosol absorption (SSA) remains to bring closure to TOA UV spectra (UV AI). A table-look-up approach is adopted for the ASHE algorithm to find the value of SSA to reproduce UV AI, given the other information about aerosols. Thus, fifteen BBS aerosol optical property models, covering wide ranges of SSA and AOT spectral dependence, are employed in the ASHE algorithm. These BBS optical property models are based on the aerosol models used for TOMS and MODIS aerosol retrievals [*Torres et al.*, 1998; *Hsu et al.*, 2004, 2006]. TOA radiances are then simulated using the Dave radiative transfer code [*Dave*, 1972] to generate look-up tables (LUTs) of UV AI for 10 solar zenith angles, 16 viewing zenith angles, 10 relative azimuth angles, 9 AOT values (0.0–5.0 at 550 nm), and 6 ALH values (0.5 km–9.0 km). These LUTs are also used for retrieving ALH during the processes of the ASHE algorithm.

[7] The ASHE algorithm works following the steps listed below: (1) identification of BBS dominant areas within each MODIS granule, using information from the MODIS AOT and Ångström exponent as well as the corresponding UV AI from OMI; (2) collocation of ALH (from the VFM product) acquired along the CALIPSO path with MODIS and OMI over the BBS pixels determined from (1); (3) retrieval of SSA for the BBS pixels along the CALIPSO track when collocated measurements of CALIPSO, MODIS AOT and Ångström exponent and OMI UV AI are all available, by searching the pre-constructed LUTs; and (4) retrieval of ALH over the entire MODIS granule where the BBS pixels are identified, using an average of SSA derived along the CALIPSO path from (3) as a spread function via searching the LUTs.

[8] To determine the areas under influence of BBS in step (1), a scheme proposed by *Jeong and Li* [2005] to classify the dominant aerosol type, utilizing MODIS AOT and Ångström exponent together with the OMI UV AI, is applied. In brief, the UV AI is used to detect UV-absorbing aerosols (e.g., dust and BBS). Then, Ångström exponent is used to determine whether the target aerosols are mostly in coarse mode (dust) or fine mode (BBS). Minimum thresholds of AOT (0.3) at 550 nm and AI (0.7) are employed to minimize false aerosol type classification. Other thresholds for AOT, Ångström exponent and AI for detailed aerosol type(s) classification were modified from the original version [*Jeong and Li*, 2005] to account for differences in wavelengths and data characteristics and to optimize BBS detection.

[9] For steps (2) through (4), it is important to choose pixels for which the measurements from different sensors can be considered to be based on the same target. For each MODIS granule, the ASHE algorithm collocates MODIS pixels with OMI pixels to within $0.2^\circ \times 0.2^\circ$ in latitude and longitude as well as CALIPSO to within $0.1^\circ \times 0.1^\circ$. The temporal match-up windows are within $\sim$2 and $\sim$15 minutes from MODIS measurements for CALIPSO and OMI, respectively. Then, spatial variability of the ratio between OMI AI and MODIS AOT for 3×3 consecutive pixels is evaluated, and only those pixels with variability of the AI/AOT ratio less than 20% qualify for further retrieval. For those BBS pixels, SSA values are then retrieved along the CALIPSO track by searching a BBS model that can reproduce the values of OMI UV AI computed from equation (1) with the given AOT, Ångström exponent from MODIS, and CALIPSO ALH, using the aforementioned LUTs [step (3)].

[10] Once SSA values are determined along the track of CALIPSO, an average of SSA for the BBS pixels along the CALIPSO tracks within a corresponding MODIS granule is calculated [step (4)]. This value is then used as an input, together with the MODIS AOT and Ångström exponent, to derive ALH from LUTs by fitting the corresponding UV AI values. This procedure is applied to all BBS pixels (i.e., both on and outside of the CALIPSO tracks) within the MODIS granule, assuming the absorption property does not vary significantly within the same BBS plume. High spatial variability in SSA may result in a degradation of ALH estimation. However, as discussed in the next section, it turns out to be a reasonable assumption.

3. Results

[11] The ASHE algorithm has been applied to collocated and coincident measurements of MODIS/Aqua, OMI, and CALIPSO for BBS events over North America and Southeast Asia. One example of such an event, capturing wildfires over the northwestern part of the United States on August 15, 2007, is shown in Figure 1. Figure 1a is a true color image, while Figures 1b and 1c provided corresponding maps of the corresponding MODIS AOT (550 nm) and OMI UV AI. On this day, the major source region of BBS is Idaho and Montana (upper-left corner of Figure 1a) as indicated by fire pixels (red spots) reported by

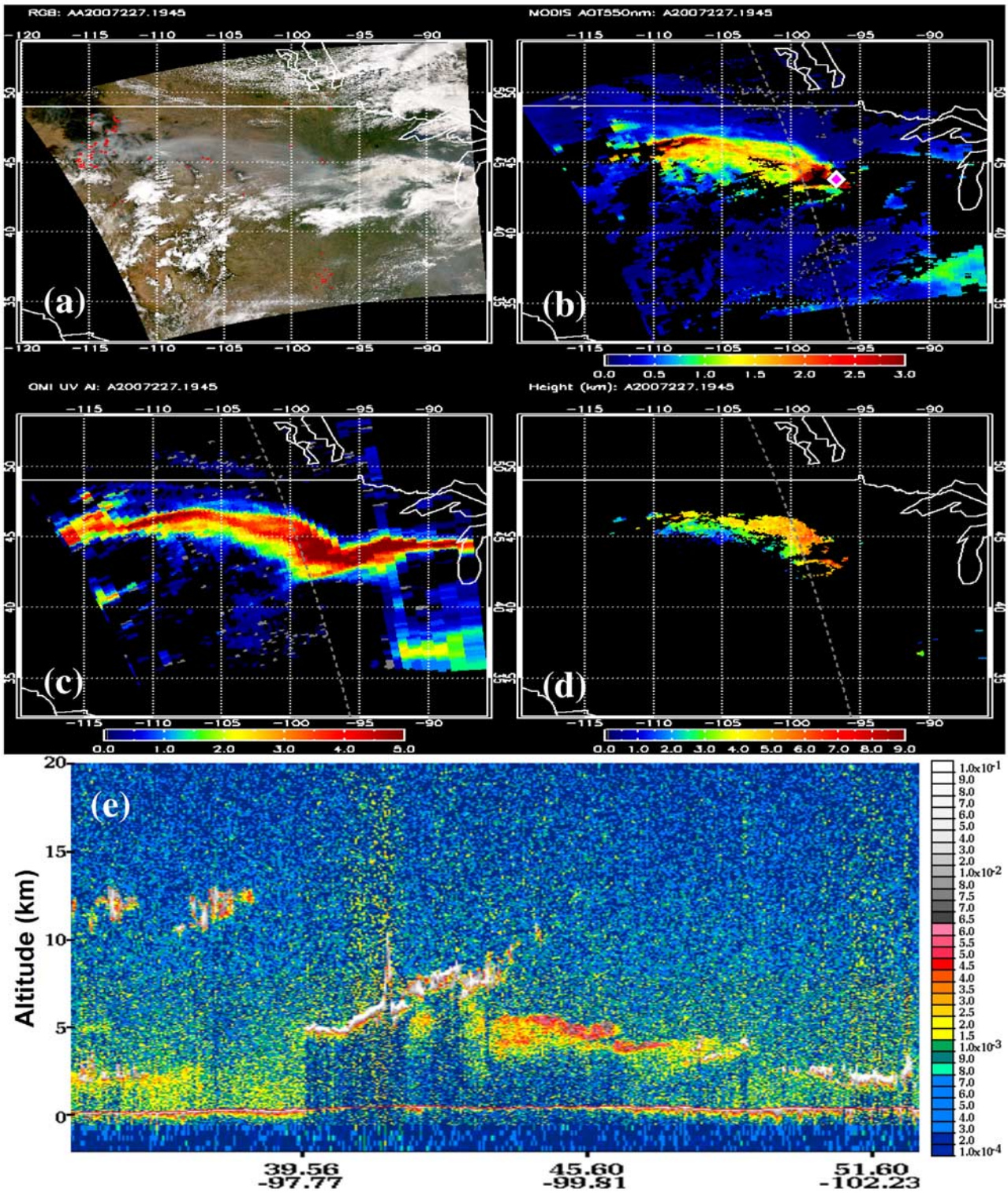

Figure 1. (a) Aqua/MODIS RGB image of a BBS event occurring at 1945 UTC on 15 Aug 2007. Red spots are fire pixels reported by the operational MODIS fire product. (b) MODIS AOT (550nm) for the same scene as shown in Figure 1a. The pink symbol shows the location of an AERONET site. (c) UV Aerosol Index from OMI for the same scene as shown in Figure 1a. (d) Aerosol Layer Height (ALH; unit in kilometers) estimated by the ASHE algorithm for the same scene as shown in Figure 1a. Gray dashed lines represent the CALIPSO track. (e) Total attenuated backscatter (532nm) profile from CALIOP along the path delineated by gray dashed lines in Figures 1b–1d.

the MODIS fire product. The areas with high UV AI are generally consistent with the distribution of MODIS AOT, except over cloudy regions (the right-hand side of Figures 1b and 1c) where high OMI AI values and no MODIS AOT values are reported, indicating the presence of BBS plumes above cloud decks. Total attenuated

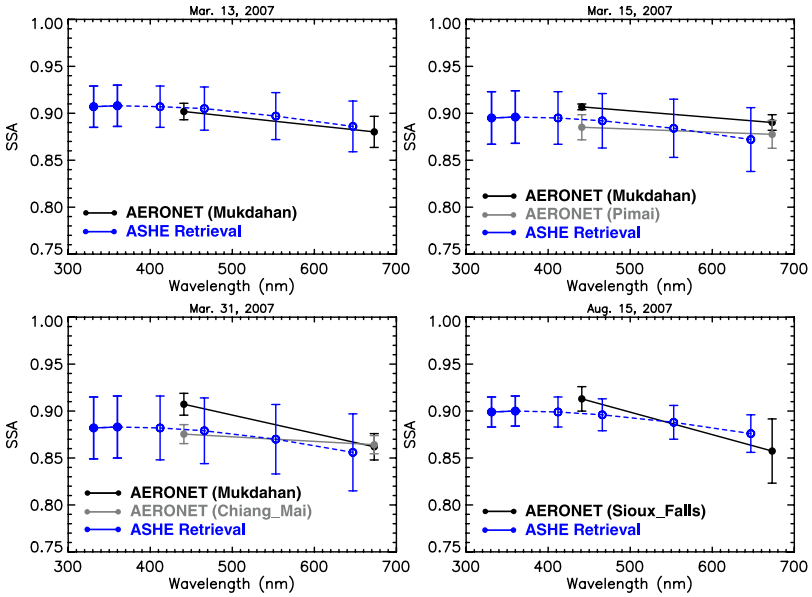

Figure 2. Comparison of SSA retrieved from the ASHE algorithm (blue lines and symbols) and AERONET SSA (black and gray lines and symbols). Provided are the average (and standard deviation) values of SSA for all qualified BBS pixels along respective CALIPSO tracks within each MODIS granule. The SSA values for wavelengths greater than 400nm are extrapolated, based on the aerosol optical property models embedded in the ASHE algorithm; therefore these are presented as open circles and dashed lines. AERONET SSA values are daily averages (and standard deviations) with AOT (at 440 nm) > 0.4. The respective AERONET sites (Mukdahan, Pimai, and Chiang_Mai in Thailand; Sioux_Falls in the United States) were under the influence of the corresponding BBS episodes in each MODIS granule.

backscatter profiles from CALIOP (Figure 1e) reveal that the BBS plumes along its track (shown as gray dashed lines in Figures 1b–1d) are located around 4–5 km above the ground. Approximately 15% of the pixels in this MODIS scene are identified as smoke-laden pixels by the ASHE algorithm [step (1)], and SSA values are estimated along the track of the CALIPSO, using the ALH derived from the CALIPSO VFM data as discussed above [steps (2)–(3)].

[12] The ASHE algorithm then uses this derived SSA as a transfer standard to extend the along-track ALH information provided by CALIPSO to the rest of the MODIS granule. The resulting map of retrieved ALH values for this Idaho wildfire is shown in Figure 1d. In order to reduce the uncertainty in the retrieved aerosol property associated with low AOT or unfavorable retrieval conditions, quality flags from the MODIS aerosol product and thresholds values for AOT and UV AI are employed to determine pixels qualified for retrieval. For example, only those pixels with MODIS AOT flagged as "Very Good" quality and with minimum AOT and UV AI values of 0.3 and 0.7 qualify for ALH retrieval. In Figure 1d, it is noted that the retrieved ALH near the source area (i.e. over northern Idaho) was relatively low (1–3 km above ground level) and rose up to 5–6 km in the downwind direction, where the BBS plume is seen over some clouds located around 5 km, as indicated by CALIPSO.

3.1. Comparisons of Derived SSA From the ASHE Algorithm With AERONET Values

[13] In order to evaluate the robustness of the ASHE algorithm, the resulting SSA values, which are used to transform the ALH information along the CALIPSO track to the entire MODIS granule, have been compared with the AERONET SSA [*Dubovik and King*, 2000], collected under the same BBS episodes. Spectral SSA between 300 nm and 700 nm from the ASHE algorithm and AERONET for four cases are provided in Figure 2. For the ASHE algorithm, only the SSA values at 331 nm and 360 nm are directly retrieved using the information from UV AI. The estimated SSA for wavelengths >400 nm are extrapolated based on aerosol models selected by the algorithm. As mentioned in the previous section, the ASHE SSA retrievals provided in Figure 2 are averages (and standard deviations as error bars) for all the qualifying BBS pixels along the respective CALIPSO tracks within each MODIS granule. The AERONET SSA values also represent averages of all the data with AOT (440 nm) greater than 0.4 for the corresponding days. In general, the magnitude and shape of spectral SSA retrievals from the ASHE algorithm show good agreement with those from the AERONET. Although this comparison may not constitute a validation since the AERONET SSA is also based on an inversion algorithm that requires assumptions of optical and physical parameters, good agreement between the two independent techniques provides a level of assurance. Such agreement also suggests that the ALH may be estimated by merging the AERONET inversions with OMI and MODIS data wherever applicable.

3.2. Self-Consistency Check

[14] In order to test the assumption whereby an averaged value of the retrieved SSA for BBS aerosols in each MODIS granule is used to estimate ALH over wide areas, we compare the ALH retrieved from the ASHE algorithm, as shown in Figure 3a, with that from the CALIPSO VFM data. Retrievals for 10 MODIS granules over North America and Southeast Asia are provided in Figure 3a. In general,

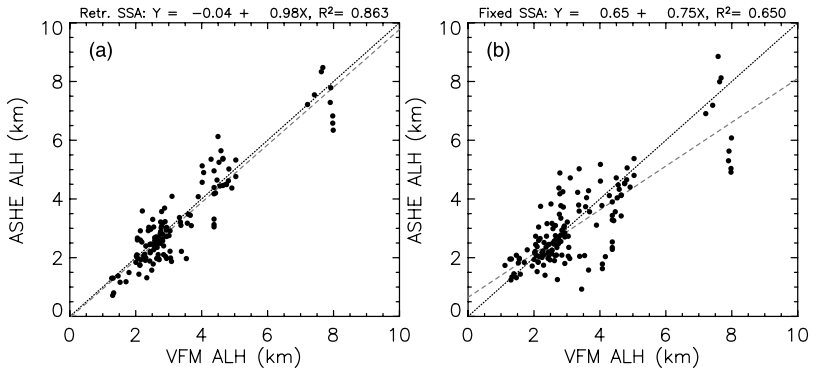

Figure 3. (a) Aerosol Layer Height (ALH) retrieved by the ASHE algorithm compared with ALH determined from the CALIPSO Level 2 Vertical Feature Mask (VFM) product, used as a validity check for the assumption of homogenous SSA values for the BBS plumes within each MODIS granule when retrieving ALH. Dotted and dashed lines stand for one-to-one and linear regression lines, respectively. (b) Similar to Figure 3a, but using only OMI and MODIS observations with a fixed assumed value (i.e., 0.90 at 360 nm) of SSA in the ASHE retrieval of ALH.

good agreement is found with a correlation coefficient (R^2) of 0.86. This indicates that ALH from CALIPSO can be extended beyond CALIPSO tracks with good confidence through the data fusion accomplished by the ASHE algorithm.

4. Simplified Approach to Derive ALH Using Only MODIS and OMI

[15] CALIPSO was launched in June 2006, while Aura and Aqua were launched in July 2004 and April 2002, respectively. Since nearly two years of collocated OMI and MODIS data are available for ALH estimation before CALIPSO data were available, the ability to estimate ALH using only two passive sensors such as MODIS and OMI is highly desirable. Also, the availability of reliable near real-time data is a critical component of field experiment planning and aerosol data assimilation for air quality models. While data downlink and processing of MODIS and OMI data are normally close to near real-time, CALIPSO data may not be available in a timely manner.

[16] In order to test the ability to obtain ALH information without CALIPSO data, we have performed tests by feeding a reasonable fixed guess of SSA (0.90 at 360 nm) into the ASHE algorithm to estimate ALH for collocated OMI and MODIS pixels. This makes the ASHE algorithm employ only steps (1) and (4) described in section 2. The results are compared with collocated ALH from CALIPSO data in Figure 3b. The correlation coefficient (R^2) between our retrieved ALH values and those of CALIPSO decreased to 0.65, but still generally indicates a reasonable agreement. The reason for the degradation can mostly be attributed to the discrepancies in SSA values between the assumed and true values over BBS events associated with different fuel types.

[17] Nevertheless, the results suggest that ALH estimation without CALIPSO data still deliver useful information in terms of separating aerosols residing in boundary layers from those aloft. Although superior ALH estimates can generally be expected from the ASHE algorithm when SSA is retrieved during the process, the simplified approach using an assumed SSA has strong potential for applications requiring near real-time ALH estimations, such as air quality forecasting and field experiment planning.

5. Concluding Remarks and Discussions

[18] A new algorithm, called ASHE, has been developed to extend the ALH information from CALIPSO along its track into more widespread areas by combining measurements from CALIOP with those from MODIS and OMI. In cases where CALIPSO data is unavailable, ALH information can still be retrieved, at a degraded but still useful level of accuracy, by merging only MODIS and OMI data. It is important to note that the ALH that we infer using the ASHE algorithm may not be interpreted as a geophysical vertical profile. Instead, it should be considered as a radiatively effective height of aerosols, which can reproduce the TOA reflectance spectra observed by OMI and MODIS, assuming Gaussian aerosol vertical distributions with a width of 1 km. Thus, retrievals will be subject to errors when BBS aerosols are present at multiple layers.

[19] Differences in pixel size and viewing geometries between MODIS and OMI can also be a potential source of errors. For example, MODIS aerosol products are derived based on radiances at 500 m resolution and AOT retrievals made only from an average of cloud-free pixels within a 10×10 km box. On the other hand, OMI has a resolution of 13×24 km and is thus more susceptible to sub-pixel clouds. These differences make ALH retrievals using merged MODIS/OMI measurements particularly challenging over regions of high variability, such as sharp edges of narrow BBS layers or small puffy BBS plumes. This problem is exacerbated when OMI is looking at the edge of swath and MODIS is at its nadir position. Aggregating the pixels for the two datasets to attain equivalent pixel size may help improve the results.

[20] Another complicated situation may occur when moderately thick BBS aerosols reside above scattered clouds. In such cases, MODIS AOT may be still available without significant cloud contamination, due to the fact that the smaller MODIS footprints allow aerosol retrievals between the clouds. But with coarser spatial resolution, OMI footprints may contain sub-pixel clouds below BBS layers, resulting in elevated signals in the UV AI due to

enhanced aerosol absorption via stronger radiative interactions among clouds, aerosols and air molecules [*Keil and Haywood*, 2003]. If such a situation happens, it would result in the underestimation of SSA for the influenced pixels. Subsequently, if an underestimated value of SSA is applied to any other uninfluenced pixel, the corresponding ALH would be underestimated. All these diverse sources of potential errors need to be taken into account in quality control procedures before a robust system of merging information from multi-platform satellite sensors can be achieved.

[21] **Acknowledgments.** This work is supported by grant from the NASA Applied Sciences Program, under L. Friedl. We thank grant PI John McHenry of Baron Advanced Meteorological Systems for useful discussions during this research. CALIPSO data were obtained from the NASA Langley Research Center Atmospheric Science Data Center. The OMI L1B data were acquired from the Goddard Earth Sciences Distributed Active Archive Center, http://disc.gsfc.nasa.gov. We thank many AERONET principal investigators and their staff for establishing and maintaining the AERONET sites used in this study. We are also grateful to the MODAPS team for producing and distributing the MODIS products.

References

Anderson, T. L., et al. (2005), An "A-Train" strategy for quantifying direct climate forcing by anthropogenic aerosols, *Bull. Am. Meteorol. Soc.*, *86*, 1795–1809.

Dave, J. V. (1972), Development of programs for computing characteristics of ultraviolet radiation, technical report, Fed. Syst. Div., Int. Bus. Mach. Corp., Gaithersburg, Md.

Dubovik, O., and M. D. King (2000), A flexible inversion algorithm for retrieval of aerosol optical properties from Sun and sky radiance measurements, *J. Geophys. Res.*, *105*, 20,673–20,696.

Herman, J. R., P. K. Bhartia, O. Torres, C. Hsu, C. Seftor, and E. Celarier (1997), Global distribution of UV-absorbing aerosols from Nimbus 7/TOMS data, *J. Geophys. Res.*, *102*, 16,911–16,922.

Hsu, N. C., J. R. Herman, P. K. Bhartia, C. J. Seftor, O. Torres, A. M. Thompson, J. F. Gleason, T. F. Eck, and B. N. Holben (1996), Detection of biomass burning smoke from TOMS measurements, *Geophys. Res. Lett.*, *23*, 745–748.

Hsu, N. C., J. R. Herman, O. Torres, B. N. Holben, D. Tanre, T. F. Eck, A. Smirnov, B. Chatenet, and F. Lavenu (1999), Comparisons of the TOMS aerosol index with Sun-photometer aerosol optical thickness: Results and applications, *J. Geophys. Res.*, *104*, 6269–6279.

Hsu, N. C., et al. (2004), Aerosol properties over bright-reflecting source regions, *IEEE Trans. Geosci. Remote Sens.*, *42*, 557–569.

Hsu, N. C., et al. (2006), Deep blue retrievals of Asian aerosol properties during ACE-Asia, *IEEE Trans. Geosci. Remote Sens.*, *44*, 3180–3195.

Jeong, M.-J., and Z. Li (2005), Quality, compatibility and synergy analyses of global aerosol products derived from the advanced very high resolution radiometer and Total Ozone Mapping Spectrometer, *J. Geophys. Res.*, *110*, D10S08, doi:10.1029/2004JD004647.

Jeong, M.-J., Z. Li, D. A. Chu, and S.-C. Tsay (2005), Quality and compatibility analyses of global aerosol products derived from the advanced very high resolution radiometer and moderate resolution imaging spectroradiometer, *J. Geophys. Res.*, *110*, D10S09, doi:10.1029/2004JD004648.

Keil, A., and J. M. Haywood (2003), Solar radiative forcing by biomass burning aerosol particles during SAFARI 2000: A case study based on measured aerosol and cloud properties, *J. Geophys. Res.*, *108*(D13), 8467, doi:10.1029/2002JD002315.

NASA (2003), Formation flying: The afternoon "A-Train" satellite constellation, *NASA Fact Sheet*, *FS-2003–1–053–GSFC*, 6 pp.

Torres, O., et al. (1998), Derivation of aerosol properties from satellite measurements of backscattered ultraviolet radiation: Theoretical basis, *J. Geophys. Res.*, *103*, 17,099–17,110.

Vaughan, M. A., et al. (2005), CALIOP algorithm theoretical basis document, part 2: Feature detection and layer properties algorithms, *Rep. PC-SCI-202*, 87 pp., NASA Langley Res. Cent., Hampton, Va.

N. C. Hsu and M.-J. Jeong, NASA Goddard Space Flight Center, Greenbelt, MD 20771, USA. (myeong-jae.jeong-1@nasa.gov)